Near-Infrared Quantum Dots and Their Delicate Synthesis, Challenging Characterization, and Exciting Potential Applications

Frank C.J.M. van Veggel

January 2014

Near-Infrared Quantum Dots, their delicate synthesis, challenging characterisation, and exciting potential applications

Frank C.J.M. van Veggel

Department of Chemistry
University of Victoria
Victoria, BC
V8W 3V6 Canada

Email: fvv@uvic.ca

Abstract

This review articles describes the progress made over the last decade and a bit on the synthesis, characterisation, and (potential) applications of quantum dots that have optical transitions in the near-infrared. It is to some extent focussed on lead chalcogenide quantum dots, because most progress has been made here. In addition, the most common characterisation techniques are briefly discussed, as well as current and future applications, such as in photovoltaic devices ("solar cells"), in light-emitting diodes, and as biolabels. I have tried to cite many reviews for further reading as way to compensate for the occasional conciseness.

Keywords: near-infrared quantum dots, synthesis, characterization, applications

Introduction

Since my first exposure to quantum chemistry during my Chemical Technology studies in the 80's in the Netherlands, I have been intrigued by quantum phenomena. I remember being impressed by at least two things during the introductory class on this topic. One is that, even with a fairly simple molecular orbital theory, the Pauli exclusion principle, and Hund's rules, ground state molecular oxygen comes out as a biradical, without any ad hoc explanation. This is not evident from a classical Lewis structure. The other is the classical "particle-in-a-box" model. If one takes a particle that only has kinetic and potential energy, then solving the Schrödinger equation with boundary conditions of infinite potential energy in three dimensions one obtains a set of solution to this differential equation that have discrete energy levels and their spacing increase as the box gets smaller. The energies are $n^2h^2/8mL^2$, with n the fundamental quantum number, h Planck's constant, m the mass of the particle, and L the length of the cubic box. This phenomenon is usually called quantum confinement in the field of (colloidal) quantum dots (and quantum rods, quantum wires, and the like). A QD is in essence a tiny piece of semiconductor that is quantum confined in three dimensions. One could also solve the "particle-in-a-box" for a spherical box.[1-2] In an analogous fashion, quantum wires have confinement in two dimensions and quantum wells in one. The length at which quantum confinement effects kick in is the Bohr radius, which was defined by Niels Bohr for "his" hydrogen model as the most probably distance between the electron and the proton. For our purpose it would be the most probable distance between the electron (in the conduction band) and the hole (in the valence band of the exciton),[3-5] the latter being defined as a bound electron-hole pair. The term quantum dot was coined by Reed *et al*. in a 1988 article for a system with quantum confinement in three dimensions.[6] Furthermore, I was intrigued by the fact that if one doesn't make the boundary condition as an infinite potential energy, then one obtains solutions that have some of the probability of finding the particle outside the box. In other words, we have a model for (electron) tunnelling, which is a phenomenon classical theories can not explain, because the postulates don't contain the essence of quantum phenomenon. These basics are now pretty standard material in any physical chemistry textbook that includes quantum chemistry.

This fascination has never disappeared, but was revived in a sense when my research took me in the direction of nanotechnology. Although I have never work on quantum well laser,[7-9] they were probably the first artefacts I read about in which a quantum phenomenon has been used. Quantum well lasers are based on the exploitation of quantum confinement in one dimension to tune the laser emission.

My "real" exposure to the work of quantum phenomenon started by working on lead(II)-based quantum dots because they can be made to emit in the near-infrared, typically defined roughly between 800 and 3000 nm. Initially, the interest was focused on the telecommunication window, between 1300 and 1700, with a particular effort on C-band around 1550 nm. The C in C-band stands for conventional, because that was the first window that became available for telecommunication, which in my view was the co-evolution of two major developments. The first was the production of high optical glass fibers of high quality, i.e. low scatter and absorption. The second was the development of Er^{3+}-Doped Fiber Amplifiers, EDFAs.[10-12] It happens that Er^{3+} has an optical transition at 1550 nm that has a very high quantum yield and a very long-lived lasing excited state. As a matter of fact, there are not that many alternatives in this frequency range (see below). Over time, an interest also develop towards optical imaging of biological systems. More on both will be discussed in detail below.

As compared to the field of quantum dots that have optical transition in the UV-visible, in particular the field of Cd^{2+}-based quantum dots (QDs) and the like[13], the field of near-infrared quantum dots (NIR-QDs) is younger and as a consequence less mature. However, I will argue that a lot of progress has been reported over the last decade or so, in particular on the Pb^{2+}-based chalcogenides (i.e. PbS, PbSe, and PbTe QDs). This is probably because of several reasons. The first is that the syntheses of NIR-QDs, often initially mimicked on the cadmium chalcogenides, have been improved upon over the years. The second is that characterization techniques, such as electron microscopy-based ones, and other advanced ones, e.g. synchrotron-based analysis, have matured enormously and have become available to more and more researchers; and so has our understanding of them. Actually, without those (advanced) characterization technique we would be rather blind. The bulk band gaps of the semiconductors PbS, PbSe, and PbTe are 0.5, 0.37, and 0.26 eV, respectively.[14] The Bohr radius of PbSe is 46 nm, which

means that for nanoparticles smaller than this value, quantum confinement effect should appear, and then the term QD is justified.[15] As shown in more detail below, this small bulk band gap and large Bohr radius gives a wide tenability of the electronic states; the bulk band gap translates into a minimum (optical) transition 3.35 μm and QDs with transition well above 1000 nm have been reported. For instance, the bulk band gap of CdSe is 1.74 eV[14] and the Bohr radius is 6 nm.[15] This means that the longest optical transition one can get is about 700 nm.

This review will focus on three aspects. Firstly, I will describe current characterization technique, including electron microscopy, X-ray diffraction and scatter techniques, and synchrotron-based techniques. In the hope to makes this review also useful for colleagues new to the field, I will provide a brief summary of every technique and potential pitfalls. However, I will not cover "solid state" QDs fabricated by sophisticated deposition techniques that operate in the NIR.[16] Secondly, I will describe the current status of the synthesis of NIR-QD, with an emphasis on lead(II)-based chalcogenides. However, I will include other NIR-QDs, e.g. Ag_2S, because important progress has been reported over the last couple of years. Thirdly, I will briefly discuss (potential) application and the challenges as I see them to make them possible. In this relatively short review it is impossible to cover every aspect of these fascinating NIR QDs, so I would like to refer to some recent reviews that cover other aspects in more detail.[3,17-22] It will conclude with some general conclusions and an outlook. The latter is always tricky to do, because of the inherent unpredictability of research and I certainly will refrain from picking any "winners". Wasn't it Niels Bohr who famously remarked that "prediction is very difficult, especially about the future"?

Results and Discussion

I will first make some general remarks about common characterization techniques before I will discuss specific results of the NIR-QDs.

General Characterisation

Photoluminescent Properties

An important parameter of any photoluminescent material is the quantum yield (QY), which is defined as the ratio of the number of photons emitted divided by the number of photons absorbed, according to:

$$QY = \#photons\ emitted / \#photons\ absorbed \quad (1)$$

It is thus a measure of the number of excited states that decay radiatively, i.e. the decay leads to the emission of a photon (usually at a lower energy than the excitation energy). The other excited states are "lost" via non-radiative processes In this linear scenario, the quantum yield runs from 0 to 100%. For non-linear processes the quantum yield is defined in the same way, but then of course for a two-photon absorption followed by a one-photon emission, it would run from 0 to 50 %. Conversely, for quantum cutting, i.e. one photon in and two or more out, it would run from 0 to n × 100% with n the number of photons out.

The two most common ways to measure a QY are the relative and absolute method.[23-24] In the relative method way relates the unknown QY to a known reference QY, through the following equation:

$$QY_{sample} = QY_{ref} \times (n^2_{sample} \times I_{sample} \times A_{ref} / n^2_{ref} \times I_{ref} \times A_{sample}) \quad (2)$$

with QY_{sample} and QY_{ref} the quantum yields of sample and reference, respectively. If one cannot work in the same solvent the term n^2_{sample}/n^2_{ref} corrects for that. The other two terms are the emission intensity and the absorption, respectively. One of requirements of this method is that the unknown and reference material have a good spectral overlap of their respective photoluminescence. This immediately causes a serious problem when one wants to measure the QY of a NIR-QD, e.g. one that emits at 1550 nm, because there are no standards in this frequency range, let alone standards that have been accepted by the research community. I am naturally suspicious of relative QYs of NIR-QDs (and some more general criticism on reported QYs of NIR-QDs later). This measurement is typically done in the 90-degree configuration, with the collection of the emitted light perpendicular to the excitation light. This 90-degree configuration is used to

avoid/minimize the interference of the excitation light, but often one still wants to use appropriate filters to cut any scattered excitation light. The latter is particularly important if the excitation wavelength is close to the emission peaks. This is also important when one deals with nanoparticles or nanoparticles aggregates for they could scatter much more efficient than solutions.

The other most often used method is an absolute QY measurement using an integrating sphere. The integrating does in principle exactly what is says: it integrates all the light that enters the sphere (i.e. the excitation) and is created in the sphere (i.e. the photoluminescence) through a highly scattering coating on the inside of the sphere. The two most common coatings are $BaSO_4$ and Teflon®. The integrating sphere usually has baffles to avoid the collection of scattered light directly out of the integrating sphere into the collection path (i.e. monochromator and detector). In essence, there are only two measurements needed: one is a scan of the emission and the (remaining) excitation light and the other is a scan of the excitation light of a reference sample (that should not absorb any light and should mimic the scatter of the sample). From these two measurements, with appropriate corrections for the instrument response, one gets the number of emitted photons and the number of absorbed photons from which the official QY can be calculated according to equation (1).

For instance, we have noticed that the solvent is not a good reference if the Ln^{3+}-based upconversion nanoparticle size is larger than 30 nm.[25] In this case, we had to make a reference sample that was the same size but did not absorb the excitation light. However, with QD this is typically not an issue, because sizes are well below 10 nm. However, (dynamic) aggregation could be issue because it may lead to sizes that do scatter light much more efficiently than the reference (often the solvent for colloidal systems). The other aspect that one has to consider is to avoid re-absorptions, so the more dilute one can work, and still have reliable data, the better.

In order to avoid artefacts the scattering efficiency should be constant over the wavelength range of interest. For instance, the one-photon scattering curve for $BaSO_4$ is around 98% at 400 nm and decreases nearly linearly to 90% at about 1900 nm. In general one need to correct for this. For instance if we assume about 40 scatter events before the light escapes the integrating sphere then the efficiency is 45% (0.98^{40}) at 400 nm and

1.5% (0.90^{40}) at ~1000 nm, so if the excitation and emission wavelength are far apart, then this is not an insignificant effect. It is fair to say that most articles neglect this, but it is easy to do by measuring the instrument response function with the integrating sphere in the fluorescence spectrophotometer and a calibrated light source. We have recently done this[unpublished] and noticed that the instrument response curves are distinctly different between the "standard" ones, also known as correction files, provided by the vendor and the ones with the integrating sphere. It is fair to say that our older work used the standard curves and thus one can expect a (small?) systematic error in the data. On the other hand, if excitation and emission are fairly close together, then this systematic error is small (and maybe smaller than the experimental error and sample to sample variation). More details on both methods can be found in an excellent review by Eaton.[23]

There are other methods to measure the QY, e.g. the method based on thermal lensing,[26-27] but these are much less common than the two discussed above. This is maybe due to the fact that these are not readily implemented on standard fluorescence spectrophotometers or the fact that more optical expertise is needed to acquire and analyse the data.

There is one method that is officially not a QY yield measurement, but in principle only a proxy of it. This is the method of dividing the measured (averaged) life time of the excited state by the radiative life time, i.e. the life time in the absence of any non-radiative process, so:

$$QY = \tau_{measured} / \tau_{radiative} \qquad (3)$$

In general the radiative life time is not known but can be approximated by a life time measurement at very low temperatures where one assumes that all non-radiative processes have effectively been shut down. In some case, the radiative life times can be calculated as is the case for the trivalent lanthanides through the Judd-Ofelt theory.[28-29] There is an excellent recommendation by Eaton on how to record and report life times.[30] At times one also reads the term quantum efficiency as synonym for quantum yield, but this should be avoided, because quantum efficiency is typically done on an energy scale and not a photon counting scale.

The excited state life time is another parameter that informs us about the (nano)material we made. For semiconductors it is typically the lifetime of the excited state with the electron at the bottom of the conduction band, with its Boltzmann distribution which is a function of among others the absolute temperature, and the hole near the top of the valence band. This excited state is created by the absorption of a photon (or two or more) that promotes an electron to the conduction band and when its energy is higher than the energy of the emitted photon, it typically falls down very fast to the bottom of the conduction band through internal conversion processes.

However, not all absorption events lead to an exciton and not all excitons lead to an emitted photon, because there are competing processes. For instance, an electron high up in the conduction band could induce Auger processes[31] or the exciton could be quenched due to phonon coupling[32]. Obviously, these competing processes make the QY of PL less than 100%.

Common Characterisation Techniques

Of the many other characterization techniques available to us these days, electron microscopy, X-ray Diffraction, (synchrotron-based) X-ray Photo-electron Spectroscopy, Dynamic Light Scattering, zeta-potential analysis are probably the most prevalent. Others that are fairly common are Small Angle X-ray Scattering. A "cousin" of SAXS is Small Angle Neutron Scattering (SANS) , but this is not often used, likely because one needs a nuclear reactor for this work.

Electron microscopy is a very powerful characterization tool because it can be done in many different modes, which finds its origin in the many physical processes that can occur when a sample is hit with an energetic beam of electrons. Figure 1 summarizes the various processes.

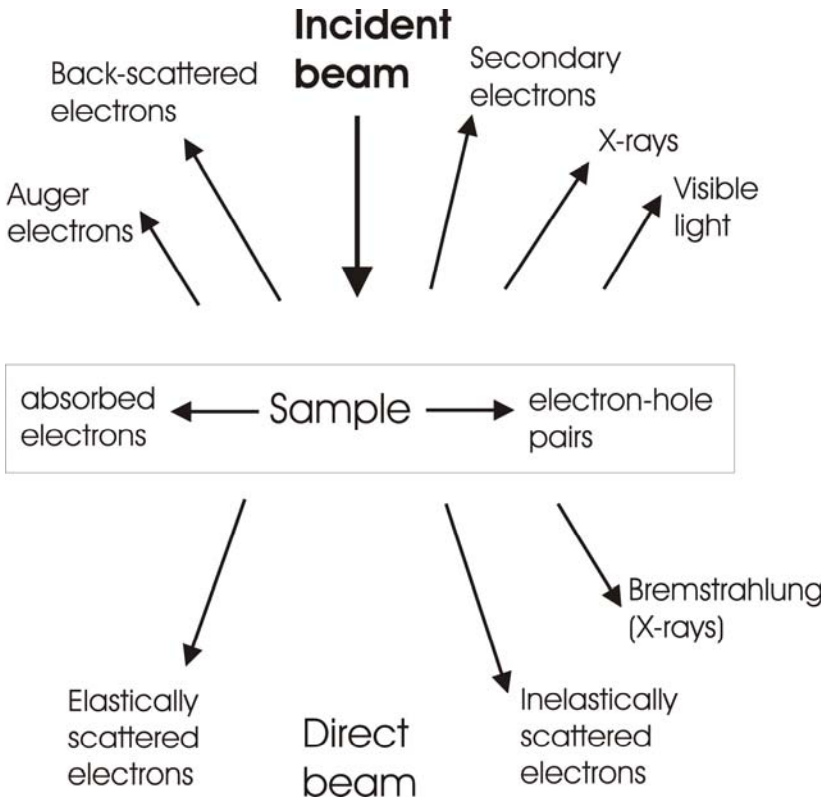

Figure 1. Processes that can occur when a sample is hot with a beam of energetic electrons, after.[33]

The basic measurement in a transmission EM (TEM) is based on the fact that there is a difference between the intensities of the incident and direct beam (the bright field) precisely because of all the other processes. Thus, if a QD is in the path of the beam it leads to a contrast and it would appear as a dark spot in the image. If the resolution of the TEM is high enough one could see lattice fringes, because of interference effects, from which information regarding the crystal structure can be obtained. Of course, an amorphous nanoparticles will not show these lattice fringes. The images of lower magnification are most often used to produce histograms of the binned size vs. the frequency (of 50-100 particles); from it the average size and standard deviation are then calculated. However, many articles are rather vague on how many and how they measured the particle sizes. Although absolutely monodisperse samples, i.e. samples with nanoparticles of only one size, do not exist, the term is used for samples with a size dispersion of less than 5%. This at least seems the accepted value. Selected Area Electron

Diffraction (SAED) is fairly standard on most advanced EMs and provides information about the crystal phase of the sample. The secondary electrons are used in a Scanning EM (SEM). A scanning TEM (STEM) scans the incident beam to create the image. The element-specific X-rays that result are used for the elemental analysis of the ensemble or of individual nanoparticles, and are referred to as Energy Dispersive Spectroscopy (EDS) or Energy Dispersive X-ray spectroscopy (EDX). EDS/EDX are also generated by incident X-rays in X-ray fluorescence instruments; these X-rays are the secondary ones. The *elastically* scattered electrons, i.e. those scattered electrons that have not lost energy through interaction with the sample, form the basis of Z-contrast imaging, also know as High-Angle Annular Dark Field imaging (HAADF), because the scatter angle is to a first-order approximation proportional to square of the atomic number Z. The part "dark field" in HAADF refers to the fact that this is a area outside the bright field (= direct beam), but clearly one still detects electrons to generate the image; the term dark field is thus a bit misleading. The *inelastically* scattered electrons, i.e. those scattered electrons that have lost some energy through interaction with the sample, form the basis of Electron Energy-Loss Spectroscopy (EELS) and is also an element-specific phenomenon. Another implementation of EELS mapping is energy-filtered TEM (EF-TEM), in which one uses a filter that only allows the passage of electron with a certain kinetic energy. In EELS mapping one actually measures part of an EELS spectrum, from which the map is then created through the software. The elemental mapping of a nanoparticles can be done in line scan mode or across the whole particle, for instance.[34-35] Obviously the latter mode requires the nanoparticles to be extremely stable in the electron beam. EDS and EELS are particularly powerful techniques in a STEM, because it allows the investigation of single (core-shell) QDs. The other phenomena in Figure 1 are not (often) used to characterize QDs.

X-ray power diffraction (XRD) is of course based on Bragg's law and is valuable for phase identification (with comparison to data base phases of bulk materials) and crystallite size determination (through the Scherrer equation).[36] In general the crystallite size corresponds well with the QD size (as determined from TEM measurements), but this is of course not a guarantee.

X-ray Photo-electron Spectroscopy (XPS)[37] starts with shining an X-ray beam onto the sample (in high vacuum) that leads to absorption of it with a concurrent ejection of a photo-electron from one of the core orbitals. The kinetic energy of this photo-electron is measured in an analyzer, which is them used to calculate the binding energy of that photo-electron through: $E_{binding} = E_{X\text{-}ray} - E_{kinetic} - \Phi$. The term Φ is the work function of the instrument (and would require calibration) and is usually small compared to the other energies (hundreds to thousands of eVs). The binding energy is element and oxidation specific. The fact that it is element specific of course stems from the fact that the (core) electron have different binding energies, depending on the specific element. The fact that it is also oxidation specific is easy to see. If the oxidation state increases, let's say from 0 to +2, then all remaining electrons are bound a bit more strongly, because there is less electron-electron repulsion, and thus the photo-electron has a slightly higher binding energy and would give a slightly lower kinetic energy for the same incident X-ray energy. XPS is also known as Electron Spectroscopy for Chemical Analysis (ESCA), but this term seems to be less and less used. As I will show below, XPS becomes especially powerful when done at a synchrotron, because very monochromatic X-rays over a very large energy range with incredible intensities are available. A synchrotron does a lot more for us, because it produces electromagnetic radiation from hard gamma rays to far into the infrared, so a host of other techniques are possible. A synchrotron has a sweet of end stations, the beam lines, that allow all kind of measurements depending on the required energy range.

Dynamic Light Scattering (DLS), also known as photon correlation spectroscopy or quasi-elastic light scattering, is a technique based on Rayleigh scattering, that provides information of the hydrodynamic radius of the colloidal nanoparticles. It finds is basis in the fluctuations of scattered light from a laser as function of time, because nanoparticles diffuse in and out the focus of the laser beam (through their Brownian motion).[38]

Zeta-potential analysis provides a measure of the overall surface charge of the nanoparticles. The colloidal solution is placed in an electric field that changes the diffusion of the overall charged nanoparticles, which is measured by a change in the scattered light of a laser.[39]

Small Angle X-ray Scattering (SAXS) provides information of nanoparticles size and shape, and ensemble dispersity. SAXS, because it is based on the scatter of X-rays, is particularly sensitive to elements with high atomic numbers, so information of the "soft" organic stabilising (mono)layer is hard to get. The scattering intensity is recorded as a function of the scattering vector, which is the characteristic scattering length scale in reciprocal space. The strength of this analysis stems from the fitting of the data against a model (e.g. a sphere, a core-shell, a cylinder, etc. as model). Many standard software packages can do this and through the NIST in the USA quite a large number of macros are now available. Contrary to SAXS, Small Angle Neutron Scattering (SANS) is very appropriate to study the "soft" organic stabilising (mono)layer because neutrons are well scattered by hydrogen atoms. Similarly, insight is obtained by fitting the data against a model.

Some General Remarks on their Colloidal Synthesis

On paper the synthesis, from a chemist's point of view, looks extremely simple, with the vast majority of QD syntheses following the "hot-injection" method, which has mostly been developed for the cadmium chalcogenide QDs and copied and adapted for other QDs, for instance.[13,40-45] The hot-injection method is based on the concept of adding one of the reactants very fast into the hot reaction mixture, having all the other reactants, stabilisers, and (non-)coordinating solvents, thus creating a supersaturation which leads to the formation of a burst of nuclei that then grow, preferably all with the same rate, over time to the desired size. The approach is based on the LaMer model[46-47], which however has recently been challenged.[48-49] In essence one wants all of this last reagent to be injected at t = 0. It is quite typical to use the reaction time and temperature as the parameter to control size, but also the concentration and the salt to stabiliser ratio play a role. At this particular time, the reaction is then quickly quenched and worked up further to isolate the QDs, wash away excess stabilisers, etc. This indeed sounds very simple and should be doable on "lab scale", but as so often, the devil is in the details. For instance, what is fast in the step of "fast injection"? This is often not specified in the experimental section, so new researchers to the field have to learn this by trial and error. Many other devilish details exist, with some annoying hard to control (and often leading to a low

reproducibility). I will now make some general remarks based on our 10 year experience with PbS- and PbSe-based syntheses (but I think the is some general truth in them regarding other NIR QDs). Maybe the most notorious one is the purity of the reactants and other chemicals used in the synthesis. TOP, very often used to solubilise elemental selenium and tellurium, is contaminated with dialkylphosphines which play a crucial role in the formation of PbSe NIR QDs, as shown in a detailed study by Klimov and co-workers.[50] Even buying this chemical from the same vendor is no guarantee, as we and no doubt many others have observed. Another culprit for low reproducibility is oleic acid (typically 90% pure and the other 10% likely other fatty acids). The natural source of oleic acid and the way it is purified are of course the major sources of inconsistency. This may suggest that the other fatty acid are more than just innocent bystanders in the synthesis. Yet another variable stems from the Pb^{2+} salt that is used, most often PbO and $Pb(OAc)_2$ with oleic acid as the organic stabiliser. Very often I read acetate abbreviated as "Ac", but this is incorrect, because in organic chemistry Ac stands for acyl, i.e. the $CH_3C(O)$ moiety, and not for acetate, i.e. $CH_3C(O)O$, abbreviated as OAc (or AcO). It seems reasonable to assume that both react with the excess oleic acid to form $Pb(oleate)_2$ as the reactive lead source, so one also forms water and acetic acid, respectively, which are often evaporated off. However, especially for water, it far from clear if this is done to completion and it is my impression that the small amounts remaining do change the outcome. This small-scale synthesis presents other challenges with respect to reproducibility if one wants to scale it up to grams, tens of grams, and beyond. The fast injection obviously becomes problematic in large scale reactions, but also controlling the temperature of big reaction flasks or reactors is far from trivial, as well is the quenching of the reactions mixture to stop the further growth of the QDs.

It is well-know from the cadmium chalcogenide field that the optical properties are compromised by surface defects, such as vacancies and dangling bonds, because one terminated a crystal structure in three dimensions to make a QD. Stabilisers or ligands do help mitigate these issues, but the most effective way is to grow a shell of another semiconductor around the QD, thus generating core-shell structures. The choice of the shell material is often a commensurate semiconductor. If this semiconductor has a higher

band gap than the core semiconductor and if this gap "spans" the core gap, then one has a so-called type I core-shell QD (see Figure 2).

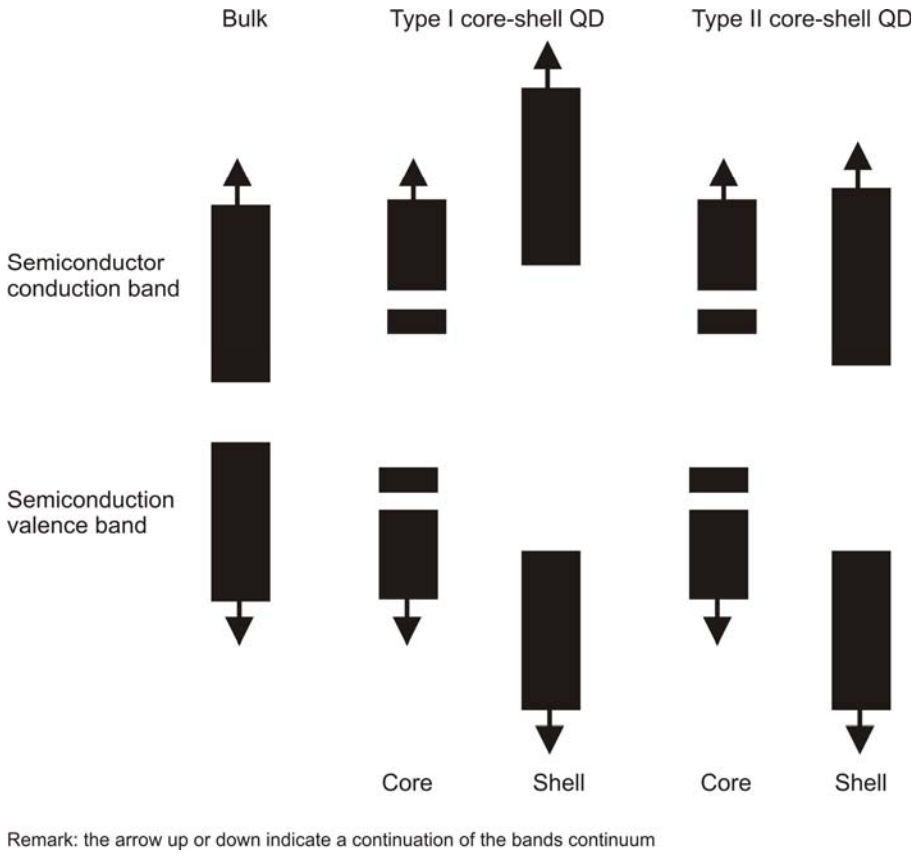

Figure 2: the band structure of a bulk semiconductor (left), a type I core-shell QD (middle), and type II core-shell QD (right).

The exciton after a one-photon absorption is most confined to the core, in other words the wavefunction of hole and electron are mostly confined to the core. This is the preferred scenario if one wants a photon-in photon-out process. If for instance the conduction band is lower in energy than the conduction band of the core, then the electron is mostly confined to the shell (and the hole to the core). Such a combination is referred to as type-II. Other scenarios not leading to type-I are of course possible, with for instance one subgroup referred to as quasi-type-II.[31] This is not desirable for a photon-in photon-out process, because the two wavefunctions have less overlap and thus the probability of radiative recombination, and consequently the non-radiative processes become (more) competitive. This could be advantageous for solar cell application,

because here one wants to extract the charge carriers. i.e. electron and hole. However, the extraction of the hole, in the core, may not necessarily be efficient. Other architectures of the two semiconductors may be better in this respect.

PbX (X = S, Se, or Te) based NIR Quantum Dots

X = Se

As far as I am aware, the first seminal report of a wet-chemical synthesis of colloidal PbSe quantum dots is by Murray *et al.* in 2001.[51] They synthesised PbSe QDs by injection of a solution of lead oleate and TOP-Se in TOP into stirred diphenyl ether at 150 ^{o}C. They tuned the reaction conditions to get QD sizes of 3.5 to 15 nm, as determined by TEM. The size range gives the exciton absorption feature from about 2200 (for the largest size) to about 1200 nm (for the smallest size), with clear higher energy features indicative of high quality samples (i.e. samples with a low size dispersion). They also used XRD and SAXS to characterise their QD samples, the latter to determine the structure of the superlattice upon their assembly in two dimensions. This was then followed by work by Guyot-Sionnest and co-workers[52] and Kraus *et al.*[53] Krauss *et al.* also reported ultrasmall PbSe QDs with exciton absorptions down to ~700 nm (and relative QY of up to 90%).[54] The PbSe and PbS QDs have an intriguing electronic structure.[55-57] If one uses a Pb(II) salt and elemental selenium as the precursor, then there must be a reduction step of the selenium happening (if one takes PbSe as an ionic compound). It is tempting to take TOP as the one-electron redactor because nearly all syntheses use the TOP-Se adduct in the reaction. However, Klimov *et al.* have shown that dialkyl phosphines are more likely to play this role.[58] Similarly, amines could function as one-electron reductors and the role of oleyl amine in nanoparticles synthesis has recently been reviewed by Maourdikoudis and Liz-Marzán.[59] As mentioned in the general section on their synthesis, the stabilising ligands play a crucial role, not only in the colloidal stability but also in the formation of them. For instance, Baek *et al.* showed a ligand effect on the size of PbSe QDs.[60] In a similar spirit Murray and co-workers have shown that different phosphine-selenium adducts lead to different PbSe nanostructures, i.e. from QDs to QRs (quantum rods).[61] Small QDs appear as spheres in the TEM, maybe because the crystal facets are ill-defined, but this remains a bit surprising to me, given the fact that

PbX have a cubic crystal structure. Maybe the influence of the stabilising ligands "override" this innate structure. Bigger PbSe QDs are more cubes than spheres and other shapes have been reported.[62-63] The lead(II) acetate and TOP-Se seems to be the most often used precursors for PbSe QDs, for instance see[64-68], "but variation on this theme" have appeared.[69] Koole *et al.* published a detail study on the optical confinement properties of PbSe QDs.[70] Ternary lead chalcogenide QDs, $PbSe_xTe_{1-x}$, PbS_xTe_{1-x}, $PbSe_xSe_{1-x}$ have been reported by Smith *et al.*[71]

X = S

Hines and Scholes published some impressive work on PbS QDs in 2003.[72] They reacted lead(II) acetate and TMS_2S [bis(trimethylsily) sulphide] in oleic acid and octadecene to arrive at sizes that give exciton absorption features from about 800 to 1800 nm. Maybe not too surprising for such an early report, the size dispersion are in the range of 10-15% and PL QYs of around 20%. Ozin and co-workers showed the extinction coefficient to be size dependent.[73] In 2008, we showed that using TOP in the synthesis and further careful optimization of the reaction conditions and reagent ratios, the size dispersion can be narrowed down to 3.7% with a PL FWHM (full width at half maximum) of the exciton emission of 49 meV (a Stokes shift of only 7 meV) and absolute QYs as high as 80% for the QD PL between 1100 and 1300 nm.[74] This QY value allows me another remark, also made in this article. The very high QY was measured for 4 of the 10 batches we made of QDs that were very close in size and size dispersion. The other 6 batches were lower. It would not come as a shock to colleagues familiar with the fact that these reactions remain finicky and that (on occasion) we made batches that were simply lousy in terms of QY. The larger QDs, with their PL peak between 1300 and 1600 nm, had QYs of 40-60%. If one reads an article with (NIR) QDs that have very high PL QYs and it reports only one measured, one should assume that this is not necessarily "THE" number. This and other remarks I made above simply show that the reproducibility of these syntheses is not (yet?) great. Ligand effects have also been reported by Moreels *et al.*[75]

Acharya *et al.* synthesised PbS, from lead(II) nitrate, thiourea in hexadecylamine and TOPO (trioctyl phosphine oxide) with sizes 2.3 to 10 nm for photovoltaic applications.[76] From performance studies in photovoltaic devices, with ITO and TiO_2/Al

as electrodes, they conclude that PbS QDs of 3.5 nm, corresponding to a energy gap of 3.5 eV, is the optimal size.

Kanatzidis and co-workers reported the use of tin, a group-12 element in $Pb_{2-x}Sn_xS_2$ ternary compound.[77] Lead(II) acetate, tin(II) acetate, elemental sulphur in a mixture of TOP, oleyl amine, oleic acid, and octadecene were use to synthesise these QDs. The onset of near-infrared absorption is higher than for the PbS "parent" compound, i.e. 0.52-057 vs. 0.44 eV, with a size ~6 to 11 nm for the former. These ternary compounds are stable up to ~300 ^oC, upon which they decompose in the two binary compounds.

Weiss and co-workers showed that PbS QDs can be oxidised with tetracyanoquinodimethane (TCNQ).[78]

X = Te

In contrast to the sulphides and selenides, less work has been reported on lead telluride. Murray an co-workers reported the synthesis of PbTe QDs and their assembly in superlattices.[79] The QDs were made in an analogous way as the PbSe QDs by reacting lead(II) acetate with TOP-Te. They tuned their size from 4 to 14 nm, with the biggest one cubic in shape. The exciton absorption was observed from ~1900 to almost 2400 nm, with concomitant Stokes shifted PL. The small size dispersion (<5%) leads to close-packed superlattices.

A recent development is work by Kanatzidis and co-workers on the incorporation of antimony,[80] a group-13 element. They used TOP-Se, lead(II) acetate, antimony acetate in a mixture of oleic acid and oleyl amine to synthesise $Pb_mSb_{2n}Te_{m+3n}$ QDs with m = 2, 3, 4, 6, 8, and 10, and n = 1 and 2. Sizes based on TEM and XRD range from 10 to 12 nm, but it is fair to mention that the size dispersion is still modest. The bandgap are in the range of 0.43 eV, as determined from infrared absorption spectra. These ternary QDs decompose at temperatures of 300 ^oC into PbTe and Sb_2Te_3, consistent with the fact that the bulk ternary compounds are not stable.

A somewhat uncommon synthesis route has been used by Chubilleau and co-workers employing laser fragmentation to make PbTe QDs, but the size dispersion is large.[81] Other work on PbTe QDs has appeared.[69,82-87]

Core-shell PbX-based NIR Quantum Dots

The general approach to make a (type-I or II) core-shell QD is to grow (epitaxially) a semiconductor shell on the core QD. This method has been very successful for the Cd^{2+}-based QDs, but has only been of limited success for the PbX cores. To my knowledge only the combination of PbSe-PbS has been reported following this "classical" approach, with the first report by Lifshitz and collaborators.[88-92] Our entry into this field was the reproduction of this synthesis for we were interested in the question if this core-shell QD is colloidally and photochemically more stable.[93] We concluded that the Pbse-PbS core-shell QDs are rather of the type-II than the type-I. This was followed later by Lifshitz and co-workers[94-95] Work by others in this system has also appeared.[96] It is somewhat surprising that no other semiconductor have been grown (epitaxially) on PbSe, because there are potential materials with a good lattice match, e.g. EuS. Several of my post-doctoral fellows have spent considerable effort on this. We had cases where the TEM images look promising for shell formation but the PL was absent. I am convinced that my group has not been the only one trying this method and the absence of reports may hint to the fact that the PL properties of the PbX core are very sensitive to the reaction conditions, i.e. they don't seem to withstand temperature well above 150 ^{o}C. The first successful synthesis of PbSe-CdSe was by the groups of Hollingsworth and Klimov in 2008.[97] They performed a cation exchange, i.e. swapping some Pb^{2+} for Cd^{2+}, to make PbSe-CdSe "core-shell QDs". Careful inspection of the TEMs in the main text and supporting information shows that the nanoparticles may not all be proper core-shell QDs; proper in the sence that the shell is equally think everywhere around the core. This is something the authors must have concluded as well, because they call their nanomaterials heterostructures and not core-shell QDs. In any case, this article was the first demonstration that other than PbSe-PbS core-shell QDs could be made. This cation-exchange approach is based on the seminal work by Alivisatos *et al.* who were the first to demonstrate this process in ionic nanostructures.[98] An excellent review on this matter has appeared.[42]

Inspired by this result, we decided to improve on these results and have shown that with proper fine tuning of the synthesis, one can make well defined PbSe-CdSe core-

shell QDs.[99] In this article we employ a large variety of characterization techniques, i.e. (HR-)TEM, HAADF, EF-TEM, XRD, synchrotron-based XPS, SAXS, and SANS. In summary these data show that (i) the PbSe core is centred in the core-shell structure, i.e. a fairly uniform CdSe had formed, (ii) the PbSe-CdSe interface is very sharp, only a few monolayers, and (iii) in toluene the stabilising oleic acid monolayer is heavily solvated. We noticed that the core and core-shell QDs are very sensitive to beam damage in the electron microscope. We have observed that in line scans sometimes the nanoparticles is split in two and sometimes simply ablated. Consequently, we always measure the bright field image after we have done HAADF, EELS mapping, or other measurements in which the sample is exposed to the electron beam for considerable time (which could be as short as 30 sec.). Figure 3 shows an example of a HR-TEM image of a number of core-shell QDs that have clear lattice fringes and contrast between the core and shell.

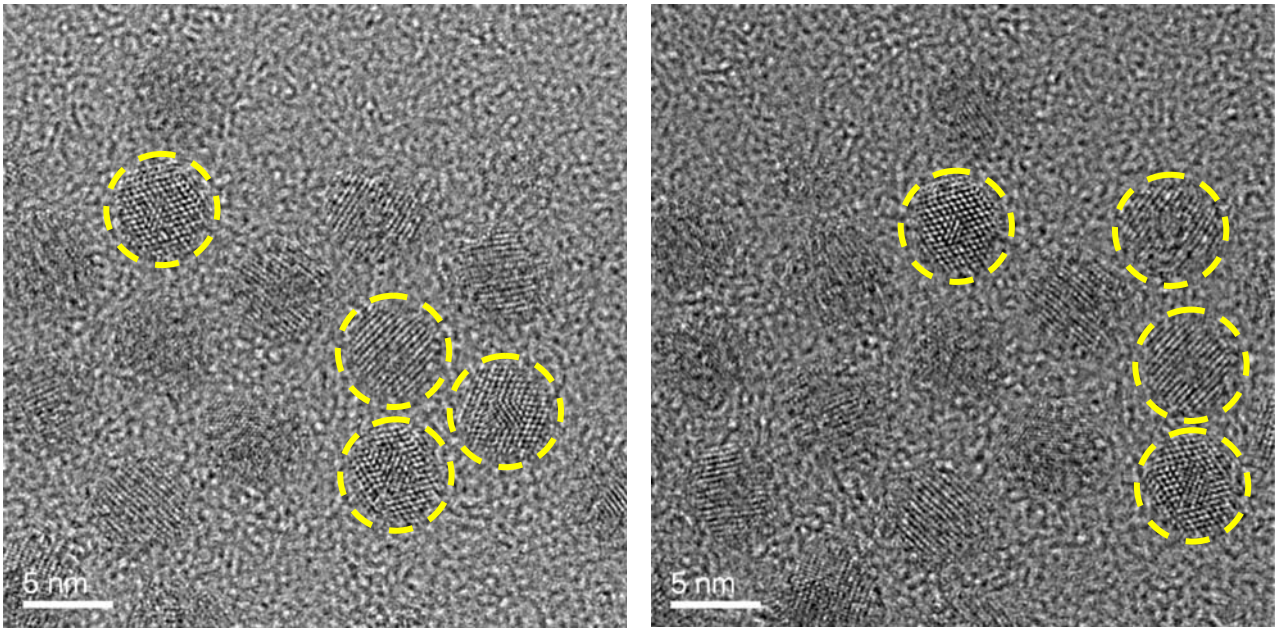

Figure 3: HR-TEM images of PbSe/CdSe core/shell QDs (λ_{abs} = 1150 nm). Circled particles show clear contrast between core and shell materials. The initial PbSe core precursor QDs had λ_{abs} = 1590 nm. Cation exchange reaction performed at 105 ^{o}C for 25 minutes. Reproduced with permission from the American Chemical Society, copyright 2012.[99]

It may be tempting to derive the shell thickness from these images, but this is not possible because one does not know if the focal plane is actually at the centre of the QD. The lead map by EF-TEM and the corresponding bright field image after the mapping are reproduced in Figure 4.

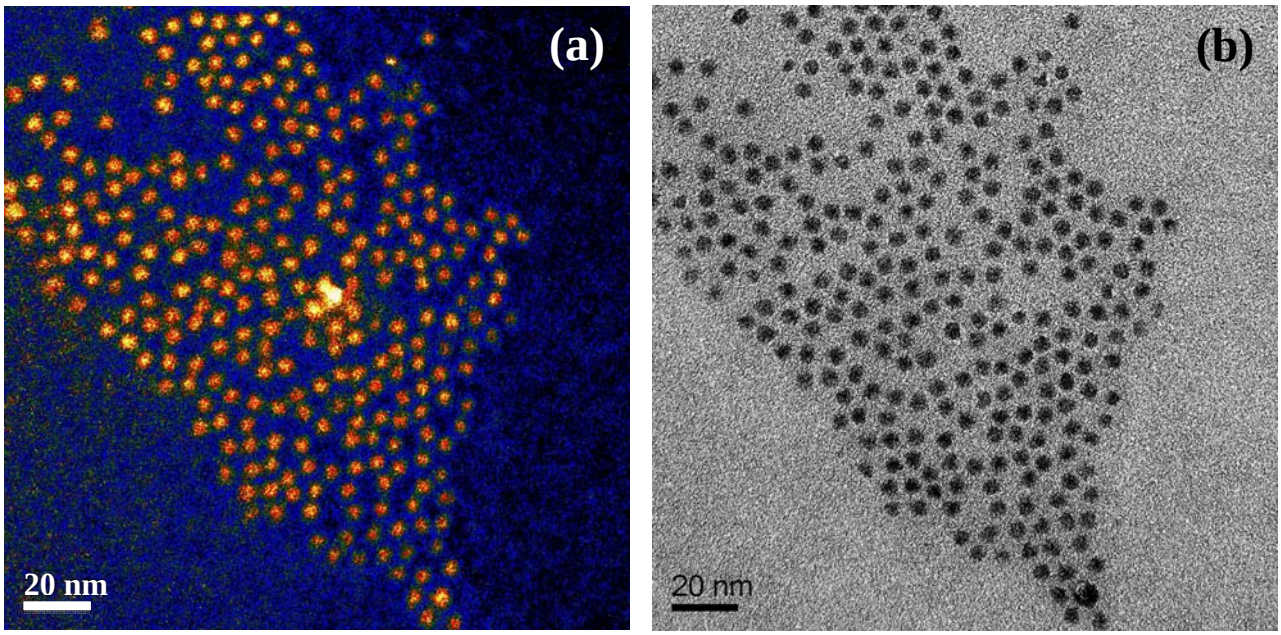

Figure 4: (a) Pb map by EF-TEM imaging of PbSe/CdSe core/shell QDs. **(b)** Bright-field image of the same core/shell particles measured *after* the EF-TEM image. The QDs are the same batch as those presented in Figure 3. Reproduced with permission from the American Chemical Society, copyright 2012.[99]

This shows that most of the QDs had survived the mapping (taking a couple of minutes), but it also shows that some (cluster?) of QDs roughly in the centre of image is gone in the bright field image; it had been ablated by the electron beam. We also provided strong evidence that the lead map is centred on the selenium map, which is consistent with a proper core-shell QD. Particularly informative are the high resolution data we measured at the Canadian Light Source, a third-generation synchrotron. Besides the very high resolution and high brilliance, a synchrotron also offers the advantage of tuneable X-rays. The latter allows one to probe (mainly) the surface of the sample with low energy X-rays

and probe deeper with high energy X-rays. This phenomenon finds its origin in the mean free path of the kinetic photo-electron that is generated after the absorption of the incident X-ray photon. These data show (Figure 5), among others, that there is a lead-containing surface species, attributed to lead(II) oleate and/or PbO, and that there is a thin interface of alloyed $Pb_{1-x}Cd_xSe$.

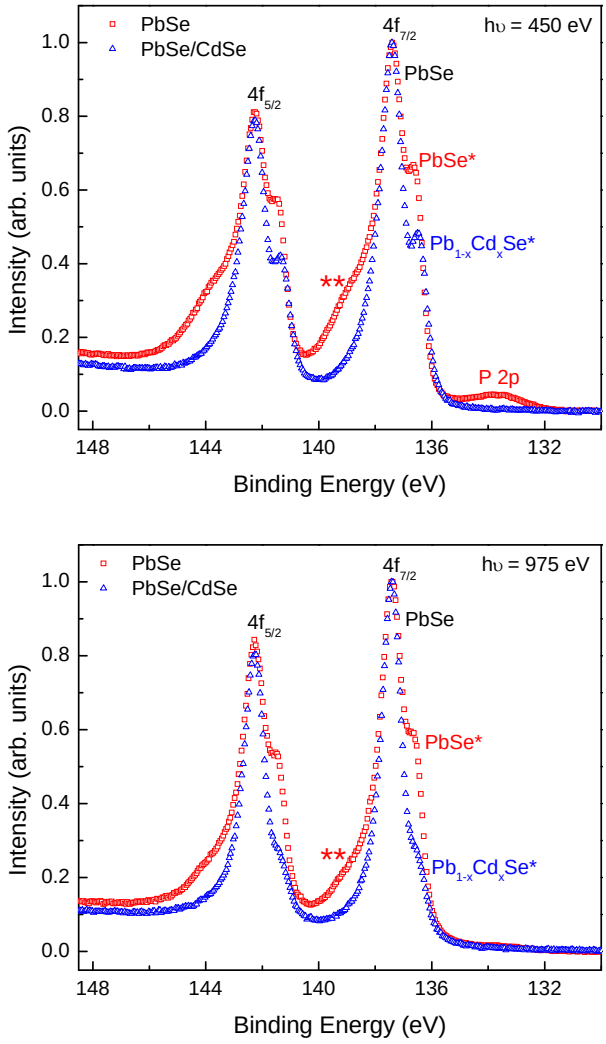

Figure 5: HR-XPS spectra of Pb 4f photo-emission peaks at two different photon energies. The ** peaks are attributed to Pb-oleates and PbO on the surface of the PbSe QDs. The calculated IMFP values are ~0.9 nm and ~2.0 nm for the 450 eV and 975 eV photon energies, respectively. Cation exchange reaction performed at 80 ^{o}C for 25 minutes. PbSe/CdSe QDs λ_{abs} = 1276 nm (initial PbSe QDs λ_{abs} = 1513 nm). Reproduced with permission from the American Chemical Society, copyright 2012.[99]

We have consistently found that the cation to anion ratio is larger than one, consistent with lead(II) oleates and cadmium oleates as the stabilising monolayer for core and core-shell QDs, respectively. Grodzińska *et al.* reported a dual emission of PbSe-CdSe core-shell QDs which is ascribed to inter-valley coupling between the L-points.[100] In another article by the same groups, De Geyter *et al.* reported a 4-fold smaller oscillator strength for the PL of the core-shell vs. the core QDs, which implies that the electron wave function is delocalised in the shell, a point supported by calculations.[101] However, because this a minor effect, they conclude that the emission from lower states are fundamentally different than the absorption transition.

Subsequently, we reported a detailed analysis of the temperature-dependent absorption and PL.[102-103] The core-shell QDs have a higher energy barrier for non-radiative decay than the corresponding PbSe QDs. The Stokes shift of the PbSe PL is dominated by thermalisation of the exciton population, and there is clear evidence for a temperature-independent broadening associated with surface states. Other solvent effects have been described.[104] Not unexpectedly, the cation-exchange process is very dependent on the exact conditions and anisotropy has been reported by Casavola *et al*.[105] In a recent paper we also discuss the stark differences in the optical properties of 2D and 3D thin films.[106] In collaboration with my colleague Jeff Young at the University of British Columbia in Vancouver, we have a long-standing interest in the integration of NIR-QDs and photonic devices that operate in the telecommunication window, with the ultimate goal to contribute to quantum computing and quantum cryptography applications. To this goal we have published that NIR-QDs can couple to the microcavities of silicon-based photonic devices, which is potentially a scalable approach.[107] Because of the fact that such approaches have the NIR-QDs necessarily in a "dry state", studying their optical properties is needed and we have shown a saturation behaviour when they are pumped in a photonic device.[108]

Other NIR Quantum Dots

The next section briefly describes the progress that has been made with NIR quantum dots that are not based on the lead chalcogenides. Bawendi *et al*. developed InAs-based

NIR quantum for bio-imaging (bulk band gap is 0.36 eV[14] and the Bohr radius is 34 nm[15]). Their first report on this was in 2005 on $InAs_xP_{1-x}$/InP/ZnSe core-shell-shell NIR quantum dots.[109] The reactants for the core synthesis were $In(OAc)_3$, TMS_3As, and TMS_3P in a mixture of oleic acid and octadecene. The first shell was made from $In(OAc)_3$ and TMS_3P and the second shell from Et_2Zn and TOP-Se. A ligand exchange reaction was then used with an "oligomeric phosphine"[110] to make them dispersible in a PBS buffer at pH = 7.0. The PL was tuned from ~600 to ~800 nm. They imaged the sentinel lymph node of rats with the NIR labels injected subdermally. Based on the time evolution of the P/As ratio they conclude that the phosphine source is more reactive than the arsenic source, so the centre of the core is richer in phosphine than arsenic. $CuInSe_2$ (bulk band gap is 0.92 eV[14] and the Borh radious is 7.5 nm[111]) NIR quantum dots were then reported with PL tunability from ~650 to close to 1000 nm, which were made from TMS_2Se, CuI, and InI_3 as the precursors in a mixture of TOP and oleyl amine.[112] The relatively broad PL is (in part) attributed to the size dispersion. Core-shell InAs-ZnCdS NIR quantum dots, with PL between 700 and 800 nm, were used to image HeLa cells and a tumour with these QDs having an advantage over visible QD (i.e. CdSe-CdS) that light from deeper in the tissue could be observed.[113] However, the penetration depth of 200 μm is still relatively modest. In a 2009 article they focus on the biodistribution and clearance of InAs-ZnS core-shell NIR QDs.[114] This article shows that the nature, charge, and polarity of the stabilising organic corona plays a major factor in the biodistribution and clearance. Ag_2Te core and Ag_2Te-ZnS core-shell NIR QDs have been reported by Ma and co-workers, made from $AgNO_3$, Te, $Zn(OAc)_2$, and thiourea (Ag_2S, Ag_2Se, and Ag_2Te have bulk band gaps of 0.90, 0.15, 0.67 eV, respectively).[115] They report PL emissions that cover a range from 900 to almost 1400, which are clearly composed of at least two peaks, which may find its origin in the very large size dispersion. They report relative QYs of up to 5.6%. Ag_2Se (Bohr radius is NIR QDs 2.9 nm[116]) for the second biological window, roughly between 1000 and 1400 nm, have been reported by Zhu *et al*.[117] These NIR QDs also show very broad PL profiles, which most certainly due to the large size dispersion as evidenced from the TEM images. They synthesised these NIR QDs from AgOAc and TOP-Se in octadecene as solvent. A detailed investigations has been reported by Langevin *et al*. on the size dependence of the PL of β-Ag_2Se NIR QDs,

made from AgTFA or AgOAc and Se as the sources.[118] A somewhat different approach has recently been published to get colloidal NIR QDs.[119] Millstone and co-workers show that gold-copper alloys, from $HAuCl_4$, $Cu(NO_3)_2$, and $NaBH_4$ (as the reductant), can be made with dual-peak PL between 800 and 1200 nm. I wonder if this is a true exciton emission or a surface plasmon related emission; in any case fascinating results. The biodistribution and clearance of CdTe NIR QDs has been studied, showing that they are initially accumulated in the liver, spleen, and lungs, but eventually in the liver and kidneys.[120]

Surface Modification Strategies

A common strategy to alter the physical properties of nanoparticles is to perform post-synthesis changes to the stabilising monolayer, such as silica coating, reactions on the actual ligands, ligand exchange reactions, and intercalation processes with amphiphilic low molecular weight ligands or polymers. A slightly different tack was chosen by Robinson and co-workers, who stripped off the ligands from PbS and CdSe QDs with Na_2S that lead to very closely packed hexagonal superstructures.[121] One of the main objectives is to make QDs dispersible in aqueous media, a necessity if one wants to perform biological studies and approaches in which one assembles them through oligonucleotide base pairing. Colvin and co-workers used 11-mercaptoundecanoic acid to transfer PbSe QDs to water.[122] Hyun and co-workers exchanged the surface oleates with carboxylic acids, bearing a terminal thiol or amine group, to arrive at water-dispersible PbS and PbSe QDs.[123] Sargent and co-workers used 1-mercaptoundec-yl-)tetra(ethylene glycol) to transfer oleate capped PbS QYs to HEPS, TRIS, and PBS buffers with a PL QY of 26%.[124] Lifshitz and co-workers used 2-aminoethanol to make PbSe QDs water dispersible.[125] Lin *et al.* used poly(acrylic acid) to transfer PbS QDs to water.[126] An intercalation process based on hydrophobic interactions between the oleate monolayer and the alkyl chains of an amphiphilic polymer has been reported by Ma and co-workers.[127-129] They modified poly(maleicanhydride-1-*alt*-octadecene) (PMAO) with HO-terminated polyethylene glycol to synthesise an amphiphilic polyemer of which the alkyl chains intercalate with the oleates on the QD surface and the polyethylene glycol units provide water dispersibility. To some extent all the above approaches have some

drawbacks, such as shift of the PL peak upon transfer, decrease of the PL QY, colloidal instability in water and more importantly in pH buffers. However, building on these results, we investigated four strategies to transfer oleate-capped QDs to water and pH buffers.[130] We tested: (i) silica coating; (ii) ligand exchange with PVP (polyvinyl pyrrolidone)[131]; (iii) PEG-oleate intercalation;[132] and modified PMAO intercalation. The first method worked, but the PL was totally gone, in contrast to another report.[133] The second method suffered from the same PL loss. The third and fourth method gave excellent results, especially the fourth one. Cross-linking the derivatised PMAO with a triamine[134] gave excellent long-term colloidal stability with virtually no shift in the PL peak position for up to 7 month.

A wider view on Applications

In the above I have mentioned a few (potential) applications as they relate directly to my own current interests. However, NIR QDs have attracted interest also for several other applications, one among which their use as photon harvesters and charge creators for photovoltaics ("solar cells").[135-141] For instance, Trevisan *et al.* reported on the use of PbS QDs as a way to absorb near-infrared photons and generate hydrogen.[142] Other work with PbS QDs in photovoltaic devices has also appeared.[143] Alivisatos and co-workers reported an photovoltaic device efficiency of 4.6% with PbSe QDs of 1 to 3 nm.[144] Scholes and co-workers have reported on PbS QDs in a polymer-based photovoltaic device.[145] An aspect that has hotly been debated over the last years is the exploitation of multi-exciton generation (MEG) as a way to boost the efficiency of photovoltaic devices If the energy of the absorbed photon is larger than twice the minimum energy gap, then the "excess" energy could in principle be used to create another exciton, leading to a bi-exciton. This bi-exciton could then lead to 4 charge carriers in the device, i.e. two electron and two holes. The colleagues in the field seem to argue over many aspect related to MEG in QDs, not least among which are the validity of the (sophisticated) techniques, consistency among them, the minimum photon energy required, and the quantum yield. I have followed the debate with great interest, but I don't think a consensus has been reached. I'd like to refer the interested reader to some very recent reviews on this topic.[146-151] The wider use of colloidal NIR-QDs in light-emitting diodes

(LEDs) is predicted to "be around the corner"[152] and the concept has been demonstrated with PbSe QDs[153-154] and with PbS QDs.[155-156] In all these applications the interplay of the various interfaces play a crucial role in device performance and for some excellent reviews please see.[157-158]

An area that is in my view underdeveloped is their use as optical biolabels for deep-tissue imaging.[159] There could be several reasons for that. One is that it has been very challenging to make them colloidally and optically stable in pH buffers, a prerequisite for any biological study. Another could be, that the hard ware, in particular with respect to detectors, on (non-linear) microscopes is not available. Most highly sensitive detectors quickly die around 800 nm and not many NIR-QD have been reported to emit efficiently below 900 nm. I have a Hamamatsu NIR-PMT that measures up to 1700 nm, which is arguably the most sensitive detector in this frequency range. However, it is still about an order of magnitude less sensitive than my Peltier-cooled red-sensitive PMT (Hamamatsu R928P model)). In addition, it has a very large dark current, even at -80 ^{o}C, and the noise level is also fairly high (several thousand counts per second). Advantages of these NIR-QD for deep-tissue imaging could be: (i) tuneable PL emission (for "easy" multiplexing); (ii) high two-photon absorption cross section;[160] (iii) deep penetration of excitation and emission light, for they are both in the near-infrared where tissue is more transparent than to UV-Vis light; (iv) high optical sectioning because of the non-linear excitation; (v) high brightness, because of efficient absorption, high PL QY, and relatively short PL life time (on the order of microseconds). I am optimistic that such NIR-QDs will outperform the much trumped Ln^{3+}-doped upconversion nanoparticles.[132,161]

The exciton dynamics, whether one wants "photons out" or "charge carriers out", obviously play a crucial role in all of the above applications, see.[32,162-166]

Finally, I'd like to point here to some fascinating work by Murray, whom I regard as one of the pillars in this field, and co-workers on the self-assembly of nanoparticles and quantum dots[167-170] and other applications.[171-173] In equally high esteem I have the work by Lifshitz and co-workers, some of whose work has been cited, but it is impossible to do full justice, see for instance for some recent work.[174-180] This is not to say that I don't appreciate the work by others. Of very recent date is the beautiful work of

Vanmaekelbergh and co-workers on PbSe QD low-dimensional superlattices with very precise geometric control.[181]

Conclusions and Outlook

I think it is fair to conclude that the PbX-based core and core-shell QDs have reached a fair level of maturity, both in terms of their synthesis as their characterisation. The other mentioned NIR QDs will no doubt mature over the next decade. It also seems reasonable to assume that their application will grow and that device performance will increase over time. I also expect some interesting work to appear, not only from my own lab, on their use as biolabels (e.g. for deep tissue imaging).

Acknowledgements

For the research that has come out of my lab that is cited here I would like to acknowledge the financial support from the Canada Foundation for Innovation (CFI), the British Columbia Knowledge Development Fund (BCKDF), Natural Science and Engineering Research Council of Canada (NSERC) for their financial support. In addition, my gratitude goes to all those co-workers and collaborators who have been involved in this and whose names appear in the citations.

Biographical sketch

After an MEng degree in 1986 from the University of Twente in the Netherlands, he obtained his Ph.D. *summa cum laude* there in 1990. After a short stint at Akzo, he returned to the academia. Two 2002 paradigm-shifting articles show colloidal Ln^{3+}-based nanoparticles with near-infrared luminescence. In 2002 he accepted a Tier II Canada Research Chair at the University of Victoria, renewed in 2007. Current research is on nanoparticles ranging from Ln^{3+}-doped, semiconductor, and superparamagnetic.

References

(1) Klimov, V. I. *Nanocrystal Quantum Dots*; Taylor and Francis Group, LLC: Boca Raton, 2010.
(2) Gaponenko, S. V. *Optical Properties of Semiconductor Nanocrystals*; Cambridge University Press: New York, 1998.
(3) Scholes, G. D.; Rumbles, G. *Nat. Mater.* **2006**, *5*, 683-696.
(4) Brus, L. *J. Phys. Chem.* **1986**, *90*, 2555-2560.
(5) Alivisatos, A. P. *Science* **1996**, *271*, 933-937.
(6) Reed, M. A.; Randall, J. N.; Aggarwal, R. J.; Matyi, R. J.; Moore, T. M.; Wetsel, A. E. *Phys. Rev. Lett.* **1988**, *60*, 535-537.
(7) Hofstetter, D.; Faist, J. *Solid-State Mid-Infrared Laser Sources* **2003**, *89*, 61-96.
(8) Mishurnyi, V. A.; de Anda, F.; Elyukhin, V. A.; Hernandez, I. C. *Crit. Rev. Solid State Mat. Sci.* **2006**, *31*, 1-13.
(9) Pecharroman-Gallego, R. *Laser Eng.* **2013**, *24*, 277-314.
(10) Desurvire, E. *Erbium-Doped Fiber Amplifiers: Principles and Applications*; Wiley: New York, 1994.
(11) Miniscalco, W. J. *J. Lightwave Technol.* **1991**, *9*, 234-250.
(12) Polman, A.; van Veggel, F. C. J. M. *J. Opt. Soc. Am. B-Opt. Phys.* **2004**, *21*, 871-892.
(13) Smith, A. M.; Nie, S. M. *Acc. Chem. Res.* **2010**, *43*, 190-200.
(14) Lide, D. R. *Handbook of Chemistry and Physics*; 78th ed.; CRC press: Boca Raton, 1997-1998.
(15) Wise, F. W. *Acc. Chem. Res.* **2000**, *33*, 773-780.
(16) Dalacu, D.; Reimer, M. E.; Frederick, S.; Kun, D.; Lapointe, J.; Poole, P. J.; Aers, G. C.; Williams, R. L.; McKinnon, W. R.; Korkusinski, M.; Hawrylak, P. *Laser Photon. Rev.* **2010**, *4*, 283-299.
(17) Rogach, A. L.; Eychmüller, A.; Hickey, S. G.; Kershaw, S. V. *Small* **2007**, *3*, 536-557.
(18) Cassette, E.; Helle, M.; Bezdetnaya, L.; Marchal, F.; Dubertret, B.; Pons, T. *Adv. Drug Deliv. Rev.* **2013**, *65*, 719-731.
(19) Gao, J. H.; Chen, X. Y.; Cheng, Z. *Curr. Top. Med. Chem.* **2010**, *10*, 1147-1157.
(20) Frangioni, J. V. *Curr. Opin. Chem. Biol.* **2003**, *7*, 626-634.
(21) Ma, Q. A.; Su, X. G. *Analyst* **2010**, *135*, 1867-1877.
(22) Aswathy, R. G.; Yoshida, Y.; Maekawa, T.; Kumar, D. S. *Anal. Bioanal. Chem.* **2010**, *397*, 1417-1435.
(23) Eaton, D. F. *Pure Appl. Chem.* **1988**, *60*, 1107-1114.
(24) Lakowicz, J. R. *Principles of Fluorescence Spectroscopy*; 3rd ed.; Springer: New York, 2006.
(25) Boyer, J. C.; van Veggel, F. C. J. M. *Nanoscale* **2010**, *2*, 1417-1419.
(26) Jacinto, C.; Messias, D. N.; Andrade, A. A.; Lima, S. M.; Baesso, M. L.; Catunda, T. *J. Non-cryst. Sol.* **2006**, *352*, 3582-3597.
(27) Jacinto, C.; Oliveira, S. L.; Nunes, L. A. O.; Myers, J. D.; Myers, M. J.; Catunda, T. *Phys. Rev. B* **2006**, *73*, 125107.
(28) Judd, B. R. *Phys. Rev.* **1962**, *127*, 750-761.
(29) Ofelt, G. S. *J. Chem. Phys.* **1962**, *37*, 511-520.
(30) Eaton, D. *Pure Appl. Chem.* **1990**, *62*, 1631-1648.

(31) Yoffe, A. D. *Adv. Phys.* **2001**, *50*, 1-208.
(32) Kambhampati, P. *Acc. Chem. Res.* **2011**, *44*, 1-13.
(33) Williams, D. B.; Carter, C. B. *Transmission Electron Microscopy*; 2nd ed.; Springer: New York, 2009.
(34) Abel, K. A.; Boyer, J. C.; Andrei, C. M.; van Veggel, F. C. J. M. *J. Phys. Chem. Lett.* **2011**, *2*, 185-189.
(35) Dong, C.; Korinek, A.; Blasiak, B.; Tomanek, B.; van Veggel, F. C. J. M. *Chem. Mater.* **2012**, *24*, 1297-1305.
(36) Taylor, J. C.; Hinczak, I. *Rietveld Made Easy*; Sietronics Pty Limited: Belconnen ACT 2616, 2004.
(37) Moulder, J. F.; Stickle, W. F.; Sobol, P. E.; Bomben, K. D. *Handbook of X-ray Photoelectron Spectroscopy*; Physical Electronics USA, Inc.: Chanhassen, 1995.
(38) Cao, A. *Anal. Lett.* **2003**, *36*, 3185-3225.
(39) Doane, T. L.; Chuang, C. H.; Hill, R. J.; Burda, C. *Acc. Chem. Res.* **2012**, *45*, 317-326.
(40) Malik, M. A.; Afzaal, M.; O'Brien, P. *Chem. Rev.* **2010**, *110*, 4417-4446.
(41) El-Sayed, M. A. *Acc. Chem. Res.* **2004**, *37*, 326-333.
(42) Rivest, J. B.; Jain, P. K. *Chem. Soc. Rev.* **2013**, *42*, 89-96.
(43) Donega, C. D. *Chem. Soc. Rev.* **2011**, *40*, 1512-1546.
(44) Kershaw, S. V.; Susha, A. S.; Rogach, A. L. *Chem. Soc. Rev.* **2013**, *42*, 3033-3087.
(45) Lesnyak, V.; Gaponik, N.; Eychmüller, A. *Chem. Soc. Rev.* **2013**, *42*, 2905-2929.
(46) Lamer, V. K.; Dinegar, R. H. *J. Am. Chem. Soc.* **1950**, *72*, 4847-4854.
(47) Murray, C. B.; Kagan, C. R.; Bawendi, M. G. *Annu. Rev. Mater. Sci.* **2000**, *30*, 545-610.
(48) De Yoreo, J. *Nat. Mater.* **2013**, *12*, 284-285.
(49) Baumgartner, J.; Dey, A.; Bomans, P. H. H.; Le Coadou, C.; Fratzl, P.; Sommerdijk, N. A. J. M.; Faivre, D. *Nat. Mater.* **2013**, *12*, 310-314.
(50) Joo, J.; Pietryga, J. M.; McGuire, J. A.; Jeon, S. H.; Williams, D. J.; Wang, H. L.; Klimov, V. I. *J. Am. Chem. Soc.* **2009**, *131*, 10620-10628.
(51) Murray, C. B.; Sun, S. H.; Gaschler, W.; Doyle, H.; Betley, T. A.; Kagan, C. R. *IBM J. Res. Devel.* **2001**, *45*, 47-56.
(52) Wehrenberg, B. L.; Wang, C. J.; Guyot-Sionnest, P. *J. Phys. Chem. B* **2002**, *106*, 10634-10640.
(53) Du, H.; Chen, C. L.; Krishnan, R.; Krauss, T. D.; Harbold, J. M.; Wise, F. W.; Thomas, M. G.; Silcox, J. *Nano Lett.* **2002**, *2*, 1321-1324.
(54) Evans, C. M.; Guo, L.; Peterson, J. J.; Maccagnano-Zacher, S.; Krauss, T. D. *Nano Lett.* **2008**, *8*, 2896-2899.
(55) An, J. M.; Franceschetti, A.; Dudiy, S. V.; Zunger, A. *Nano Lett.* **2006**, *6*, 2728-2735.
(56) An, J. M.; Franceschetti, A.; Zunger, A. *Nano Lett.* **2007**, *7*, 2129-2135.
(57) Kang, I.; Wise, F. W. *J. Opt. Soc. Am. B-Opt. Phys.* **1997**, *14*, 1632-1646.
(58) Joo, J.; Pietryga, J. M.; McGuire, J. A.; Jeon, S.-H.; Williams, D. J.; Wang, H. L.; Klimov, V. I. *J. Am. Chem. Soc.* **2009**, *131*, 10620-10628.
(59) Mourdikoudis, S.; Liz-Marzán, L. M. *Chem. Mater.* **2013**, *25*, 1465-1476.
(60) Baek, I. C.; Il Seok, S.; Pramanik, N. C.; Jana, S.; Lim, M. A.; Ahn, B. Y.; Lee, C. J.; Jeong, Y. J. *J. Coll. Interf. Sci.* **2007**, *310*, 163-166.

(61) Koh, W. K.; Yoon, Y.; Murray, C. B. *Chem. Mater.* **2011**, *23*, 1825-1829.
(62) Gokarna, A.; Jung, K. W.; Khanna, P. K.; Baeg, J. O.; Seok, S. I. *Bull. Korean Chem. Soc.* **2005**, *26*, 1803-1806.
(63) Khanna, P. K.; Jun, K. W.; Gokarna, A.; Baeg, J. O.; Seok, S. I. *Mater. Chem. Phys.* **2006**, *96*, 154-157.
(64) Finlayson, C. E.; Amezcua, A.; Sazio, P. J. A.; Walker, P. S.; Grossel, M. C.; Curry, R. J.; Smith, D. C.; Baumberg, J. J. *J. Mod. Opt.* **2005**, *52*, 955-964.
(65) Vasiliev, R. B.; Dorofeev, S. G.; Dirin, D. N.; Belov, D. A.; Kuznetsov, T. A. *Mendeleev Commun.* **2004**, 169-171.
(66) Houtepen, A. J.; Koole, R.; Vanmaekelbergh, D.; Meeldijk, J.; Hickey, S. G. *J. Am. Chem. Soc.* **2006**, *128*, 6792-6793.
(67) Moreels, I.; Fritzinger, B.; Martins, J. C.; Hens, Z. *J. Am. Chem. Soc.* **2008**, *130*, 15081-15086.
(68) Britt, D. K.; Yoon, Y.; Ercius, P.; Ewers, T. D.; Alivisatos, A. P. *Chem. Mater.* **2013**, *25*, 2544-2548.
(69) Niu, J. Z.; Shen, H. B.; Li, X. M.; Xu, W. W.; Wang, H. Z.; Li, L. S. *Colloid Surf. A-Physicochem. Eng. Asp.* **2012**, *406*, 38-43.
(70) Koole, R.; Allan, G.; Delerue, C.; Meijerink, A.; Vanmaekelbergh, D.; Houtepen, A. J. *Small* **2008**, *4*, 127-133.
(71) Smith, D. K.; Luther, J. M.; Semonin, O. E.; Nozik, A. J.; Beard, M. C. *ACS Nano* **2011**, *5*, 183-190.
(72) Hines, M. A.; Scholes, G. D. *Adv. Mater.* **2003**, *15*, 1844-1849.
(73) Cademartiri, L.; Montanari, E.; Calestani, G.; Migliori, A.; Guagliardi, A.; Ozin, G. A. *J. Am. Chem. Soc.* **2006**, *128*, 10337-10346.
(74) Abel, K. A.; Shan, J. N.; Boyer, J. C.; Harris, F.; van Veggel, F. C. J. M. *Chem. Mater.* **2008**, *20*, 3794-3796.
(75) Moreels, I.; Justo, Y.; De Geyter, B.; Haustraete, K.; Martins, J. C.; Hens, Z. *ACS Nano* **2011**, *5*, 2004-2012.
(76) Khan, A. H.; Thupakula, U.; Dalui, A.; Maji, S.; Debangshi, A.; Acharya, S. *J. Phys. Chem. C* **2013**, *117*, 7934-7939.
(77) Soriano, R. B.; Malliakas, C. D.; Wu, J. S.; Kanatzidis, M. G. *J. Am. Chem. Soc.* **2012**, *134*, 3228-3233.
(78) Knowles, K. E.; Malicki, M.; Parameswaran, R.; Cass, L. C.; Weiss, E. A. *J. Am. Chem. Soc.* **2013**, *135*, 7264-7271.
(79) Urban, J. J.; Talapin, D. V.; Shevchenko, E. V.; Murray, C. B. *J. Am. Chem. Soc.* **2006**, *128*, 3248-3255.
(80) Soriano, R. B.; Arachchige, I. U.; Malliakas, C. D.; Wu, J. S.; Kanatzidis, M. G. *J. Am. Chem. Soc.* **2013**, *135*, 768-774.
(81) Chubilleau, C.; Lenoir, B.; Migot, S.; Dauscher, A. *J. Coll. Interf. Sci.* **2011**, *357*, 13-17.
(82) Mokari, T. L.; Zhang, M. J.; Yang, P. D. *J. Am. Chem. Soc.* **2007**, *129*, 9864-9865.
(83) Murphy, J. E.; Beard, M. C.; Norman, A. G.; Ahrenkiel, S. P.; Johnson, J. C.; Yu, P. R.; Micic, O. I.; Ellingson, R. J.; Nozik, A. J. *J. Am. Chem. Soc.* **2006**, *128*, 3241-3247.
(84) Ko, D. K.; Murray, C. B. *ACS Nano* **2011**, *5*, 4810-4817.
(85) Lin, Z. H.; Wang, M. Q.; Wei, L. Z.; Song, X. H.; Xue, Y. H.; Yao, X. *J. Alloy. Compd.* **2011**, *509*, 5047-5049.

(86) Ziqubu, N.; Ramasamy, K.; Rajasekhar, P.; Revaprasadu, N.; O'Brien, P. *Chem. Mater.* **2010**, *22*, 3817-3819.
(87) Pan, Y.; Bai, H. Y.; Pan, L.; Li, Y. D.; Tamargo, M. C.; Sohel, M.; Lombardi, J. R. *J. Mater. Chem.* **2012**, *22*, 23593-23601.
(88) Sashchiuk, A.; Langof, L.; Chaim, R.; Lifshitz, E. *J. Cryst. Growth* **2002**, *240*, 431-438.
(89) Bartnik, A. C.; Wise, F. W.; Kigel, A.; Lifshitz, E. *Phys. Rev. B* **2007**, *75*, 245424.
(90) Brumer, M.; Kigel, A.; Amirav, L.; Sashchiuk, A.; Solomesch, O.; Tessler, N.; Lifshitz, E. *Adv. Funct. Mater.* **2005**, *15*, 1111-1116.
(91) Brumer, M.; Sirota, M.; Kigel, A.; Sashchiuk, A.; Galun, E.; Burshtein, Z.; Lifshitz, E. *Appl. Optics* **2006**, *45*, 7488-7497.
(92) Lifshitz, E.; Brumer, M.; Kigel, A.; Sashchiuk, A.; Bashouti, M.; Sirota, M.; Galun, E.; Burshtein, Z.; Le Quang, A. Q.; Ledoux-Rak, I.; Zyss, J. *J. Phys. Chem. B* **2006**, *110*, 25356-25365.
(93) Stouwdam, J. W.; Shan, J.; van Veggel, F. C. J. M.; Pattantyus-Abraham, A. G.; Young, J. F.; Raudsepp, M. *J. Phys. Chem. C* **2007**, *111*, 1086-1092.
(94) Maikov, G. I.; Vaxenburg, R.; Sashchiuk, A.; Lifshitz, E. *ACS Nano* **2010**, *4*, 6547-6556.
(95) Yanover, D.; Capek, R. K.; Rubin-Brusilovski, A.; Vaxenburg, R.; Grumbach, N.; Maikov, G. I.; Solomeshch, O.; Sashchiuk, A.; Lifshitz, E. *Chem. Mater.* **2012**, *24*, 4417-4423.
(96) Xu, J.; Ge, J. P.; Li, Y. D. *J. Phys. Chem. B* **2006**, *110*, 2497-2501.
(97) Pietryga, J. M.; Werder, D. J.; Williams, D. J.; Casson, J. L.; Schaller, R. D.; Klimov, V. I.; Hollingsworth, J. A. *J. Am. Chem. Soc.* **2008**, *130*, 4879-4885.
(98) Son, D. H.; Hughes, S. M.; Yin, Y. D.; Alivisatos, A. P. *Science* **2004**, *306*, 1009-1012.
(99) Abel, K. A.; FitzGerald, P. A.; Wang, T. Y.; Regier, T. Z.; Raudsepp, M.; Ringer, S. P.; Warr, G. G.; van Veggel, F. C. J. M. *J. Phys. Chem. C* **2012**, *116*, 3968-3978.
(100) Grodzińska, D.; Evers, W. H.; Dorland, R.; van Rijssel, J.; van Huis, M. A.; Meijerink, A.; Donegá, C. D.; Vanmaekelbergh, D. *Small* **2011**, *7*, 3493-3501.
(101) De Geyter, B.; Justo, Y.; Moreels, I.; Lambert, K.; Smet, P. F.; Van Thourhout, D.; Houtepen, A. J.; Grodzinska, D.; Donega, C. D.; Meijerink, A.; Vanmaekelbergh, D.; Hens, Z. *ACS Nano* **2011**, *5*, 58-66.
(102) Abel, K. A.; Qiao, H. J.; Young, J. F.; van Veggel, F. C. J. M. *J. Phys. Chem. Lett.* **2010**, *1*, 2334-2338.
(103) Qiao, H. J.; Abel, K. A.; van Veggel, F. C. J. M.; Young, J. F. *Phys. Rev. B* **2010**, *82*, 165435.
(104) Hassinen, A.; Moreels, I.; De Nolf, K.; Smet, P. F.; Martins, J. C.; Hens, Z. *J. Am. Chem. Soc.* **2012**, *134*, 20705-20712.
(105) Casavola, M.; van Huis, M. A.; Bals, S.; Lambert, K.; Hens, Z.; Vanmaekelbergh, D. *Chem. Mater.* **2012**, *24*, 294-302.
(106) Quintero-Torres, R.; Foell, C. A.; Pichaandi, J.; van Veggel, F. C. J. M.; Young, J. F. *Appl. Phys. Lett.* **2012**, *101*, 121904.
(107) Pattantyus-Abraham, A. G.; Qiao, H. J.; Shan, J.; Abel, K. A.; Wang, T. S.; van Veggel, F. C. J. M.; Young, J. F. *Nano Lett.* **2009**, *9*, 2849-2854.

(108) Foell, C. A.; Schelew, E.; Qiao, H. J.; Abel, K. A.; Hughes, S.; van Veggel, F. C. J. M.; Young, J. F. *Opt. Express* **2012**, *20*, 10453-10469.
(109) Kim, S. W.; Zimmer, J. P.; Ohnishi, S.; Tracy, J. B.; Frangioni, J. V.; Bawendi, M. G. *J. Am. Chem. Soc.* **2005**, *127*, 10526-10532.
(110) Kim, S.; Bawendi, M. G. *J. Am. Chem. Soc.* **2003**, *125*, 14652-14653.
(111) Yakushev, M. V.; Luckert, F.; Faugeras, C.; Karotki, A. V.; Mudryi, A. V.; Martin, R. W. *Appl. Phys. Lett.* **2010**, *97*, 152110.
(112) Allen, P. M.; Bawendi, M. G. *J. Am. Chem. Soc.* **2008**, *130*, 9240-9241.
(113) Allen, P. M.; Liu, W. H.; Chauhan, V. P.; Lee, J.; Ting, A. Y.; Fukumura, D.; Jain, R. K.; Bawendi, M. G. *J. Am. Chem. Soc.* **2010**, *132*, 470-471.
(114) Choi, H. S.; Ipe, B. I.; Misra, P.; Lee, J. H.; Bawendi, M. G.; Frangioni, J. V. *Nano Lett.* **2009**, *9*, 2354-2359.
(115) Chen, C.; He, X. W.; Gao, L.; Ma, N. *ACS Appl. Mater. Interfaces* **2013**, *5*, 1149-1155.
(116) Sahu, A.; Khare, A.; Deng, D. D.; Norris, D. J. *Chem. Commun.* **2012**, *48*, 5458-5460.
(117) Zhu, C. N.; Jiang, P.; Zhang, Z. L.; Zhu, D. L.; Tian, Z. Q.; Pang, D. W. *ACS Appl. Mater. Interfaces* **2013**, *5*, 1186-1189.
(118) Langevin, M. A.; Lachance-Quirion, D.; Ritcey, A. M.; Allen, C. N. *J. Phys. Chem. C* **2013**, *117*, 5424-5428.
(119) Andolina, C. M.; Dewar, A. C.; Smith, A. M.; Marbella, L. E.; Hartmann, M. J.; Millstone, J. E. *J. Am. Chem. Soc.* **2013**, *135*, 5266-5269.
(120) Lu, Y. M.; Su, Y. Y.; Zhou, Y. F.; Wang, J.; Peng, F.; Zhong, Y. L.; Huang, Q.; Fan, C. H.; He, Y. *Biomaterials* **2013**, *34*, 4302-4308.
(121) Zhang, H. T.; Hu, B.; Sun, L. F.; Hovden, R.; Wise, F. W.; Muller, D. A.; Robinson, R. D. *Nano Lett.* **2011**, *11*, 5356-5361.
(122) Yu, W. W.; Falkner, J. C.; Shih, B. S.; Colvin, V. L. *Chem. Mater.* **2004**, *16*, 3318-3322.
(123) Hyun, B. R.; Chen, H. Y.; Rey, D. A.; Wise, F. W.; Batt, C. A. *J. Phys. Chem. B* **2007**, *111*, 5726-5730.
(124) Hinds, S.; Myrskog, S.; Levina, L.; Koleilat, G.; Yang, J.; Kelley, S. O.; Sargent, E. H. *J. Am. Chem. Soc.* **2007**, *129*, 7218-7219.
(125) Etgar, L.; Lifshitz, E.; Tannenbaum, R. *Journal of Materials Research* **2008**, *23*, 899-903.
(126) Lin, W.; Fritz, K.; Guerin, G.; Bardajee, G. R.; Hinds, S.; Sukhovatkin, V.; Sargent, E. H.; Scholes, G. D.; Winnik, M. A. *Langmuir* **2008**, *24*, 8215-8219.
(127) Zhao, H. G.; Wang, D. F.; Zhang, T.; Chaker, M.; Ma, D. L. *Chem. Commun.* **2010**, *46*, 5301-5303.
(128) Zhao, H. G.; Wang, D. F.; Chaker, M.; Ma, D. L. *J. Phys. Chem. C* **2011**, *115*, 1620-1626.
(129) Zhao, H. G.; Chaker, M.; Ma, D. L. *Phys. Chem. Chem. Phys.* **2010**, *12*, 14754-14761.
(130) Pichaandi, J.; Abel, K. A.; Johnson, N. J. J.; van Veggel, F. C. J. M. *Chem. Mater.* **2013**, *25*, 2035-2044.
(131) Johnson, N. J. J.; Sangeetha, N. M.; Boyer, J. C.; van Veggel, F. C. J. M. *Nanoscale* **2010**, *2*, 771-777.

(132) Pichaandi, J.; Boyer, J. C.; Delaney, K. R.; van Veggel, F. C. J. M. *J. Phys. Chem. C* **2011**, *115*, 19054-19064.
(133) Wang, D.; Qian, J.; Cai, F.; He, S.; Han, S.; Mu, Y. *Nanotechnology* **2012**, *23*, 245701.
(134) Jiang, G. C.; Pichaandi, J.; Johnson, N. J. J.; Burke, R. D.; van Veggel, F. C. J. M. *Langmuir* **2012**, *28*, 3239-3247.
(135) Etgar, L. *Materials* **2013**, *6*, 445-459.
(136) Mlinar, V. *Nanotechnology* **2013**, *24*, 042001.
(137) Selinsky, R. S.; Ding, Q.; Faber, M. S.; Wright, J. C.; Jin, S. *Chem. Soc. Rev.* **2013**, *42*, 2963-2985.
(138) Kamat, P. V. *Acc. Chem. Res.* **2012**, *45*, 1906-1915.
(139) Semonin, O. E.; Luther, J. M.; Beard, M. C. *Mater. Today* **2012**, *15*, 508-515.
(140) Fu, H. Y.; Tsang, S. W. *Nanoscale* **2012**, *4*, 2187-2201.
(141) Kramer, I. J.; Sargent, E. H. *ACS Nano* **2011**, *5*, 8506-8514.
(142) Trevisan, R.; Rodenas, P.; Gonzalez-Pedro, V.; Sima, C.; Sanchez, R. S.; Barea, E. M.; Mora-Sero, I.; Fabregat-Santiago, F.; Gimenez, S. *J. Phys. Chem. Lett.* **2013**, *4*, 141-146.
(143) Giansante, C.; Carbone, L.; Giannini, C.; Altamura, D.; Ameer, Z.; Maruccio, G.; Loiudice, A.; Belviso, M. R.; Cozzoli, P. D.; Rizzo, A.; Gigli, G. *J. Phys. Chem. C* **2013**, *117*, 13305-13317.
(144) Ma, W. L.; Swisher, S. L.; Ewers, T.; Engel, J.; Ferry, V. E.; Atwater, H. A.; Alivisatos, A. P. *ACS Nano* **2011**, *5*, 8140-8147.
(145) Fritz, K. P.; Guenes, S.; Luther, J.; Kumar, S.; Saricifitci, N. S.; Scholes, G. D. *J. Photochem. Photobiol. A-Chem.* **2008**, *195*, 39-46.
(146) Zhu, X. *Acc. Chem. Res.* **2013**, *46*, 1239-1241.
(147) Shabaev, A.; Hellberg, C. S.; Efros, A. L. *Acc. Chem. Res.* **2013**, *46*, 1242-1251.
(148) Beard, M. C.; Luther, J. M.; Semonin, O. E.; Nozik, A. J. *Acc. Chem. Res.* **2013**, *46*, 1252-1260.
(149) Padilha, L. A.; Stewart, J. T.; Sandberg, R. L.; Bae, W. K.; Koh, W.-K.; Pietryga, J. M.; Klimov, V. I. *Acc. Chem. Res.* **2013**, *46*, 1261-1269.
(150) Zhu, H.; Yang, Y.; Lian, T. *Acc. Chem. Res.* **2013**, *46*, 1270-1279.
(151) Jaeger, H. M.; Hyeon-Deuk, K.; Prezhdo, O. V. *Acc. Chem. Res.* **2013**, *46*, 1280-1289.
(152) Shirasaki, Y.; Supran, G. J.; Bawendi, M. G.; Bulovic, V. *Nat. Photonics* **2013**, *7*, 13-23.
(153) Hu, W. J.; Henderson, R.; Zhang, Y.; You, G. J.; Wei, L.; Bai, Y. B.; Wang, J. K.; Xu, J. *Nanotechnology* **2012**, *23*, 375202.
(154) Choudhury, K. R.; Song, D. W.; So, F. *Org. Electron.* **2010**, *11*, 23-28.
(155) Pal, B. N.; Robel, I.; Mohite, A.; Laocharoensuk, R.; Werder, D. J.; Klimov, V. I. *Adv. Funct. Mater.* **2012**, *22*, 1741-1748.
(156) Ma, X.; Xu, F.; Benavides, J.; Cloutier, S. G. *Org. Electron.* **2012**, *13*, 525-531.
(157) Graetzel, M.; Janssen, R. A. J.; Mitzi, D. B.; Sargent, E. H. *Nature* **2012**, *488*, 304-312.
(158) He, M.; Qiu, F.; Lin, Z. *The Journal of Physical Chemistry Letters* **2013**, *4*, 1788-1796.

(159) Horton, N. G.; Wang, K.; Kobat, D.; Clark, C. G.; Wise, F. W.; Schaffer, C. B.; Xu, C. *Nat. Photonics* **2013**, *7*, 205-209.
(160) Dayal, S.; Burda, C. *J. Am. Chem. Soc.* **2008**, *130*, 2890-2891.
(161) van Veggel, F. C. J. M.; Dong, C. H.; Johnson, N. J. J.; Pichaandi, J. *Nanoscale* **2012**, *4*, 7309-7321.
(162) Hyeon-Deuk, K.; Prezhdo, O. V. *J. Phys.-Condes. Matter* **2012**, *24*, 363201.
(163) Wheeler, D. A.; Zhang, J. Z. *Adv. Mater.* **2013**, *25*, 2878-2896.
(164) Zhu, H. M.; Lian, T. Q. *Energy Environ. Sci.* **2012**, *5*, 9406-9418.
(165) Prezhdo, O. V. *Acc. Chem. Res.* **2009**, *42*, 2005-2016.
(166) Kim, J.; Wong, C. Y.; Scholes, G. D. *Acc. Chem. Res.* **2009**, *42*, 1037-1046.
(167) Murray, C. B.; Kagan, C. R.; Bawendi, M. G. *Science* **1995**, *270*, 1335-1338.
(168) Redl, F. X.; Cho, K. S.; Murray, C. B.; O'Brien, S. *Nature* **2003**, *423*, 968-971.
(169) Shevchenko, E. V.; Talapin, D. V.; Kotov, N. A.; O'Brien, S.; Murray, C. B. *Nature* **2006**, *439*, 55-59.
(170) Shevchenko, E. V.; Talapin, D. V.; O'Brien, S.; Murray, C. B. *J. Am. Chem. Soc.* **2005**, *127*, 8741-8747.
(171) Talapin, D. V.; Murray, C. B. *Science* **2005**, *310*, 86-89.
(172) Koh, W. K.; Bartnik, A. C.; Wise, F. W.; Murray, C. B. *J. Am. Chem. Soc.* **2010**, *132*, 3909-3913.
(173) Ben-Porat, C. H.; Cherniavskaya, O.; Brus, L.; Cho, K. S.; Murray, C. B. *J. Phys. Chem. A* **2004**, *108*, 7814-7819.
(174) Lifshitz, E.; Vaxenburg, R.; Maikov, G. I.; Rubin-Brusilovski, A.; Yanover, D.; Tilchin, J.; Sashchiuk, A. *Isr. J. Chem.* **2012**, *52*, 1037-1052.
(175) Grinbom, G. A.; Saraf, M.; Saguy, C.; Bartnik, A. C.; Wise, F.; Lifshitz, E. *Phys. Rev. B* **2010**, *81*, 245301.
(176) Rubin-Brusilovski, A.; Maikov, G.; Kolan, D.; Vaxenburg, R.; Tilchin, J.; Kauffmann, Y.; Sashchiuk, A.; Lifshitz, E. *J. Phys. Chem. C* **2012**, *116*, 18983-18989.
(177) Vaxenburg, R.; Lifshitz, E. *Phys. Rev. B* **2012**, *85*, 075304.
(178) Kigel, A.; Brumer, M.; Maikov, G. I.; Sashchiuk, A.; Lifshitz, E. *Small* **2009**, *5*, 1675-1681.
(179) Lifshitz, E.; Bashouti, M.; Kloper, V.; Kigel, A.; Eisen, M. S.; Berger, S. *Nano Lett.* **2003**, *3*, 857-862.
(180) Sashchiuk, A.; Amirav, L.; Bashouti, M.; Krueger, M.; Sivan, U.; Lifshitz, E. *Nano Lett.* **2004**, *4*, 159-165.
(181) Evers, W. H.; Goris, B.; Bals, S.; Casavola, M.; de Graaf, J.; van Roij, R.; Dijkstra, M.; Vanmaekelbergh, D. *Nano Lett.* **2012**, *13*, 2317-2323.